ACS OMEGA

http://pubs.acs.org/journal/acsodf

Article

Exploration of the H_2O_2 Oxidation Process and Characteristic Evaluation of Humic Acids from Two Typical Lignites

Miao Wang, Yanhong Li,* Yuanqin Zhang, Xun Hu, Qingyin Li, Yi Su, and Wenbo Zhao

Cite This: *ACS Omega* 2021, 6, 24051−24061

Read Online

ACCESS | Metrics & More | Article Recommendations

ABSTRACT: To study the effect of H_2O_2 on the content and properties of humic acids (HAs) in lignites, the experimental conditions including oxidation time, H_2O_2 concentration, and the solid−liquid ratio were investigated. Under the optimum oxidation conditions, the contents of HAs of YL and HB lignite were 45.4 and 40.9%, respectively. The HAs extracted from oxidized and raw lignites were characterized and compared. The results showed that the HAs extracted from oxidized lignites contain more total acidic groups, carboxyl groups, and aliphatic carbon than that in HAs extracted from raw lignites, and their hydrophilic−hydrophobic index value is higher and thermooxidative stability is better than those in HAs extracted from raw lignites. In addition, the composition of polycyclic aromatic hydrocarbons and fluorophore types in HAs extracted from oxidized lignites are similar to the HAs extracted from raw lignites. The results indicated that the oxidation operation can increase the content of HAs in lignites, and simultaneously increase the content of oxygen-containing functional groups and biological activity of HAs, which provided a reference for the subsequent application of HAs.

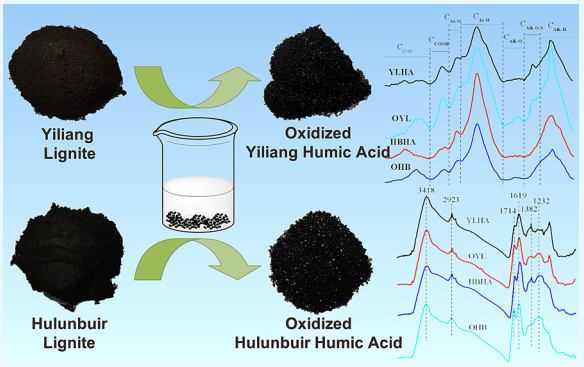

1. INTRODUCTION

Lignites are low-rank coals, and their reserves are abundant in China.[1] Generally, lignites have the characteristics of a low calorific value, low stability, high moisture, and high ash content,[2] and these shortcomings reduce their effective utilization rate as fuels in real life. The oxygen content in lignites is relatively high, and the main existing forms of oxygen-containing functional groups are hydroxyl, methoxy, phenolic hydroxyl, ether, carbonyl, and carboxyl groups,[3] and these oxygen-containing functional groups have a great influence on the chemical properties and applications of lignites. The high efficiency and clean application of lignites should be paid more attention to, including produce clean fuels, high value-added products, and carbon materials, and among which the extraction of HAs is an important way to increase the added value of lignites.

HAs are natural organic polymers that are widely found in peats, lignites, leonardites, soil, and water. The humic substances in lignites are traditionally classified into three categories according to their alkaline and acid solubility, including alkali-insoluble, alkali-soluble, and acid-insoluble, and alkali- and acid-soluble components, corresponding to humin, humic acids, and fulvic acids, respectively.[4,5] HAs are rich in a variety of oxygen-containing functional groups such as carboxyl, hydroxyl, phenolic hydroxyl, carbonyl, methoxy, and so on.[6] The chemical and physiological activities of HAs are directly related to their molecular weight, structural characteristics, and the type and number of oxygen-containing functional groups.[7] HAs have many properties, such as exchange, adsorption, complexation, and chelation with metal ions,[8,9] and are widely used in the agriculture,[10−12] industry,[13] environmental management,[14−16] medicine,[17,18] and other fields.[19,20] Therefore, research on HAs is of great significance.

HAs are insoluble under acidic conditions but can be dissolved and extracted in alkaline solutions.[4] The main methods of extracting HAs from coals are an alkaline extraction method, an acid extraction method, and a microbial dissolution method.[6,21−23] Due to the low content of free HAs in lignites, the yield is low when directly extracting HAs. To improve the yield and activity of HAs, researchers used air thermal oxidation, oxidant oxidation, mechanical activation, and other methods to pretreat lignites,[24−31] and the changes of HA structure were investigated. According to the literature,[9,24,32] oxidation of lignites by H_2O_2 to produce HAs is an important way to increase the additional utilization value of lignites.

Received: June 22, 2021
Accepted: August 17, 2021
Published: September 9, 2021

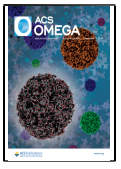

In this study, two different sources of lignites were oxidized and degraded by H_2O_2 at room temperature, and HAs were extracted by the method of NaOH dissolution and HCl precipitation. On the premise of environmental friendliness, this experiment studied the optimal process conditions for the oxidation of lignites with H_2O_2 at room temperature to increase the content of HAs. Subsequently, the difference in physicochemical properties of extracted HAs were analyzed, including proximate analysis, ultimate analysis, thermogravimetric-derivative thermogravimetry analysis (TG-DTG), and acidic functional groups analysis.[33−37] TG-DTG could be used to study the thermal properties of HAs (including thermal oxidation and thermal stability). The thermal properties and the content of acidic functional groups affect the application of HAs. Spectral analysis include Fourier transform infrared spectroscopy (FTIR), fluorescence spectroscopy (FS), NMR, and X-ray photoelectron spectroscopy (XPS), among which FTIR was often used to analyze the functional groups in HAs, NMR was used to analyze the types of carbon in HAs, XPS was used to analyze the surface elements of substances, and FS was a sensitive method for studying the structure of macromolecules.[4,7,21,23,24,38−44] The composition and properties of HAs extracted from H_2O_2 oxidized and raw lignites were studied comprehensively through a combination of multiple analysis methods. This study aimed to improve the content of HAs by H_2O_2 oxidation, provide a reference for the preparation of high-quality HAs from lignites, and provide theoretical basis for further application of HAs.

2. EXPERIMENTAL SECTION

2.1. Materials. In the experiment, two kinds of lignite from Yiliang (YL) in Yunnan (the young lignite) and Hulunbeir (HB) in Inner Mongolia (the old lignite) were used as the experimental raw materials, the total HA content in lignites was determined by the volumetric method of Chinese standard GB/T11957-2001, and the total HA contents were 27.8 and 23.9%, respectively. Before the experiment, each lignite was crushed and sieved through an 80 mesh inspection sieve. The lignites were placed in the atmosphere and dried to a constant weight, and then they were put into a sample bag and sealed for storage for later use. Hydrogen peroxide (H_2O_2) and sodium hydroxide (NaOH) were purchased from Tianjin Fengchuan Chemical Reagent Technology Co., Ltd., and hydrochloric acid (HCl, 37%) and sulfuric acid (H_2SO_4, 98%) were purchased from Chongqing Chuandong Chemical (Group) Co., Ltd. All reagents used were of analytical grade unless otherwise states.

2.2. H_2O_2 Oxidation of Lignites. The oxidation experiments were carried out as follows: The H_2O_2 aqueous solution (4, 5, 6, 7, 8, 9 wt %) was added into 2 g of YL lignite to give a final extractant to coal ratio of 1:1, 2:1, 3:1, 4:1, and 5:1 mL/g, and the mixtures reacted at room temperature for 1, 2, 3, 4, 5, 6, and 8 h. The H_2O_2 aqueous solution (5, 10, 15, 20, 25, 30 wt %) was added into 2 g of HB lignite to give a final extractant to coal ratio of 1:1, 1.5:1, 2:1, 2.5:1, 3:1, 3.5:1, and 4:1 mL/g, and these mixtures reacted at room temperature for 1, 2, 3, 4, 5, 6, 8, and 10 h. After oxidation treatment, the mixture was filtered by a Buchner funnel to separate the solid residue from the aqueous solution. The solid residue was freeze-dried and then weighed, after that measured for the HA content.

2.3. Preparation of HAs. Alkali-soluble acid separation was a common method for extraction of HAs.[4,21] The YL lignite was added sufficiently into a 0.39 mol/L NaOH solution at a liquid-solid ratio of 32:1 mL/g and reacted at room temperature for 4.1 h. The HB lignite was added sufficiently into a 0.31 mol/L NaOH solution at a ratio of 20:1 mL/g and reacted at room temperature for 5.6 h. The supernatant solution was collected by centrifugation at 6000 rpm for 5 min, and the residue was washed with deionized water three times. The supernatant was collected and filtrated with a Brinell funnel. Finally, the filtrate was acidified with HCl by pH < 2 and aged for 24 h, and then centrifuged to separate the HA (precipitate) fraction. The precipitate was slurried with distilled water and the slurry was transferred to a dialysis bag (MWCO 3500D), and then dialyzed against regularly exchanged distilled water for about 20 days. All of the extracted products were freeze-dried for further characterization and analysis, and the yield of HAs was calculated according to eq 1

$$Y_{HAs} = \frac{m_1}{m_2 \times a} \times 100\% \quad (1)$$

where m_1 corresponds to the quality of the HAs product, g; m_2 corresponds to the mass of the lignites, g; and a corresponds to the total amount ratio of HAs in lignites.

2.4. Chemical and Spectral Features Analysis. *2.4.1. Proximate and Ultimate Analysis.* The proximate analysis of lignites was determined according to the national standard of GB/T 212-2008 in China.[27,36] The moisture content was determined by air drying in a vacuum drying oven at 105−110 °C for 2 h. The ash and volatile content of the samples were automatically determined by an intelligent muffle furnace model 5E-MF6100K produced by Changsha Kaiyuan Instrument Co., Ltd. at 815 and 900 °C, respectively. The fixed carbon content could be obtained using the subtraction method.

The ultimate analyzer of a Vario macro cube model produced by Elementar, Germany, was used for ultimate analysis. C, H, N, and S were measured, respectively, and the O content was obtained by the subtraction method.

2.4.2. Determination of Oxygen-Containing Functional Groups. The total acidic functional group content was determined by the barium hydroxide method.[36,45] In the experiment, about 200 mg of the sample was suspended in a 0.05 mol/L $Ba(OH)_2$ solution (25 mL), stirred for 48 h under room temperature, filtered, and rinsed three times with distilled water without CO_2. The ion-exchanged sample was suspended in 0.1 mol/L HCl (25 mL) added in advance and titrated with 0.1 mol/L NaOH standard solution. The blank experiments were concurrently performed to calculate the total acidic groups content.

The carboxyl group content of HAs was determined by a calcium acetate method. The procedure was similar to that for total acid group determination except that the exchange solution was 0.5 mol/L $Ca(AC)_2$ instead of 0.05 mol/L $Ba(OH)_2$ (25 mL) and titrated with a 0.1 mol/L NaOH standard solution directly. The content of phenolic hydroxyl groups could be obtained by subtracting the content of carboxyl groups from the content of total acidic groups.

2.4.3. Spectroscopic Analysis. 2.4.3.1. FTIR Spectroscopy. A Fourier transform infrared spectrometer (FTIR), Nicolet iS50, was used to determine the functional groups of HAs. The KBr tablet method was used for sample measurement; the spectral resolution was 4 cm^{-1} and the spectral scanning range was 4000−500 cm^{-1}.

https://doi.org/10.1021/acsomega.1c03257
ACS Omega 2021, 6, 24051−24061

2.4.3.2. Fluorescence Spectroscopy (FS). The 10 mg/L HA solution was prepared for testing, and the solvent was NaOH (0.05 mol/L). A Hitachi F-4600 fluorophotometer was used to test the HA samples; the slit was 5 nm during the test and the scanning speed was 120 nm/min when measuring the excitation and emission wavelengths.

2.4.3.3. CP/MAS ^{13}C NMR Spectroscopy. Nuclear magnetic resonance (NMR) spectroscopy of the HAs was tested with an AVWBIII600 nuclear magnetic resonance spectroscopy instrument produced by Bruker. The test speed was 14 kHz and the resonance frequency was 150.9 MHz.

2.4.3.4. X-ray Photoelectron Spectroscopy (XPS). The multifunction scanning imaging photoelectron spectroscopy model PHI 5000 Versaprobe-II was used to analyze the surface element of HAs; the instrument power was 50 W, the voltage was 15 kV, the Al target ($h\nu$ = 1486.6 eV) was selected as the X light source, and the hemispherical pass energy analyzer was 46.95 eV, and the spectrum used was C 1s with a binding energy of 284.8 eV for correction.

2.4.3.5. TG-DTG Analysis. The thermogravimetric-derivative thermogravimetry analysis (TG-DTG) of the experimental samples was carried out with a NETZSCH STA 449F3 equipment produced by NETZSCH. The atmosphere used in the experiment was air, the heating rate was 10 °C/min, and the heating range was from 20 to 900 °C.

3. RESULTS AND DISCUSSION

3.1. Extraction Conditions of HAs. According to the single-factor experiments, the optimal oxidation conditions of HAs are obtained and are shown in Table 1. The content of HAs increases after the oxidation of H_2O_2, and it is speculated that the oxidation makes some macromolecular aromatic substances in lignites oxidize into small molecular acids.[46,47] The HAs extracted under the optimum oxidation conditions and raw lignites are used for analysis to guide the subsequent industrial production.

Table 1. Optimal Oxidation Conditions of H_2O_2 for HAs

sample	time (h)	concentration (%)	liquid-solid ratio (mL/g)	HAs content (%)
YL	3	6	3:1	45.4
HB	6	30	3:1	40.9

3.2. Proximate Analysis and Ultimate Analysis. The proximate analysis and ultimate analysis of the four HAs extracted from oxidized and raw lignites are shown in Table 2. It can be seen from the proximate analysis that the ash content of YLHA is higher. After the oxidation process, it is proved that the content of the carbon element in HAs extracted from lignites decreases after oxidation, and the content of oxygen and the O/C ratio increases, which indicates that they contain more oxygen-containing functional groups in HAs extracted from lignites after oxidation. The H/C atomic ratio can be used as an index to evaluate the aromaticity of HAs.[4,48] The larger the H/C ratio, the lower the aromaticity of the HAs. The experiment shows that the aromaticity of the four HAs is OHB > HBHA > YLHA > OYL. In addition, the O/C atomic ratio mainly reflects the content of oxygen-containing functional groups of HAs.[36,37] The content of oxygen-containing functional groups of four HAs is OYL > YLHA > OHB > HBHA. The N/C atomic ratio is assigned to the content of nitrogen in HAs, and the N/C ratio of HAs from lignite is generally less than 0.05.[48] The N/C ratios of the four HAs in the experiment are all within this range.

3.3. Determination of HAs' Functional Groups. The acidic functional groups in HAs play a significant role in the application of HAs. Therefore, the acidic functional groups of four HAs are compared and analyzed. The analysis results are shown in Table 3. It can be seen that the total acidic groups of the four HAs are OYL > OHB > YLHA > HBHA, and the content of carboxyl groups is OYL > YLHA > OHB > HBHA. The content of total acidic groups and carboxyl groups in OYL and OHB both increase, indicating that H_2O_2 oxidation can increase the active groups in HAs, thereby increasing the molecule activity of HAs.

Table 3. Determination of Functional Groups and the $f_{h/h}$ Index[a]

	functional groups (mequiv/g)		
sample	total acid	carboxyl	$f_{h/h}$
YLHA	5.84	3.74	0.50
HBHA	5.23	3.36	0.31
OYL	5.94	4.20	0.61
OHB	5.93	3.47	0.47

[a]Where mequiv/g is the capacity of ion exchange.

3.4. FTIR Spectroscopy Analysis. FTIR is used to analyze the functional groups of the four HAs, and the FTIR spectra are shown in Figure 1. It shows that the four HAs have almost the same characteristic peak positions in the infrared spectrum, which demonstrates that the types of functional groups contained are similar. It can be clearly seen from the illustration that the shoulder peak at about 1714 cm^{-1} is attributed to the stretching vibration of C=O bond in the carboxyl group.[4] Meanwhile, the peak intensities of OYL and OHB are both stronger than YLHA and HBHA, which indicates that the carboxyl content of HAs increases after oxidation. The characteristic peak at 1232 cm^{-1} is assigned to the stretching vibration of the C−O bond in esters, ethers,

Table 2. Proximate and Ultimate Analyses of HAs[a]

	proximate analysis (wt %, ad)		ultimate analysis (wt %, d)					atomic ratios		
sample	M_{ad}	A_{ad}	C	H	N	S	O	H/C	O/C	N/C
YLHA	7.33	8.09	50.23	4.64	2.04	1.64	41.46	1.11	0.62	0.03
HBHA	4.01	1.80	63.37	4.95	0.96		30.72	0.94	0.36	0.01
OYL	7.43	7.04	48.25	4.64	1.73	1.13	44.24	1.16	0.69	0.03
OHB	7.44	2.55	57.92	4.34			37.73	0.90	0.49	

[a]Where ad stands for air-dry basis and d stands for dry basis. YLHA refers to HAs in YL lignite, HBHA refers to HAs in HB lignite, OYL refers to HAs in oxidized YL lignite, and OHB refers to HAs in oxidized HB lignite.

https://doi.org/10.1021/acsomega.1c03257
ACS Omega 2021, 6, 24051−24061

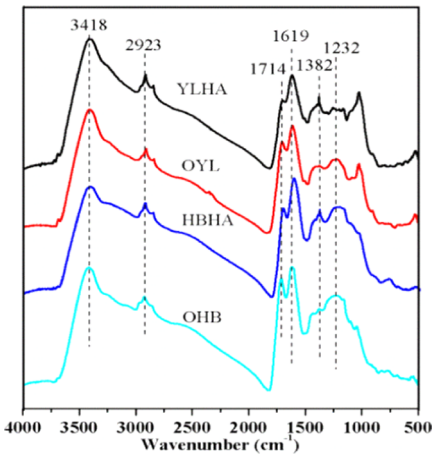

Figure 1. FTIR spectra of four HAs.

phenols, and lignin and the deformation of OH in the carboxyl group.[49,50] The peak intensity of OYL and OHB at 1232 cm^{-1} is larger than YLHA and HBHA, which indicates that the C−O content in HAs increases after oxidation, which is consistent with the results of ultimate analysis.

The FTIR spectra are fitted using a curve fitting method, and then the peaks of the correlation curve are located precisely. The content of carboxyl groups and the aromatic structure is an important index that affects the performance of HAs, so the peak fitting of the oxygen-containing functional group region (1800−1500 cm^{-1}) in the FTIR of four HAs is carried out to discuss its difference, and the fitting results are shown in Figure 2 and Table 4. It can be seen from Table 4 that the main

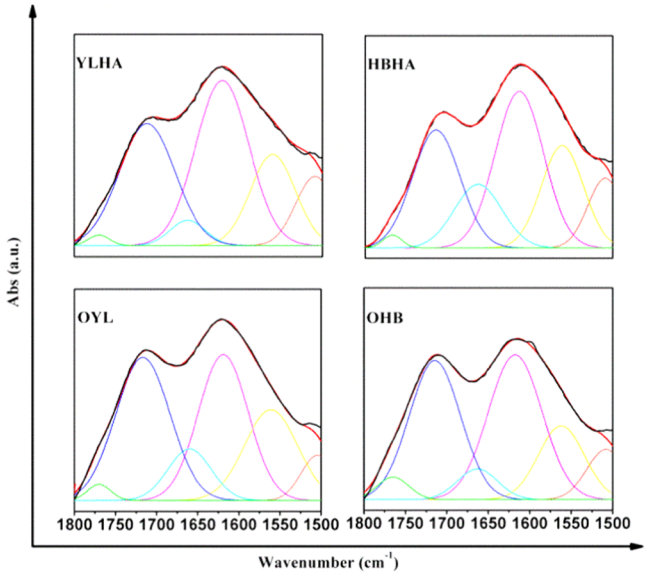

Figure 2. Fitted-peak curves of FTIR spectra of four HAs.

oxygen-containing functional groups of the four HAs are carboxyl and carbonyl, and the carboxyl contents of OYL and OHB are larger than those of YLHA and HBHA, indicating that the oxidation process increases the carboxyl content of HAs, which is consistent with the result of acidic functional group determination. It can be seen from Table 4 that the main oxygen-containing functional groups of the four HAs are carboxyl and carbonyl, and the carboxyl contents of OYL and OHB are larger than those of YLHA and HBHA, indicating that the oxidation process increases the carboxyl content of HAs, which is consistent with the results of acidic functional groups determination.

3.5. Fluorescence Spectroscopy. The electron-withdrawing groups in the HA molecules (such as carboxyl and carbonyl) can reduce the fluorescence intensity of HAs, and the electron-donating groups (such as amino, hydroxyl, methoxy, etc.) can increase the fluorescence intensity of HAs, and the presence of these oxygen-containing and nitrogen-containing functional groups can shift the fluorescence to longer wavelengths by reducing the energy difference between the ground state and the first excited state. Synchronous fluorescence spectroscopy can reduce the overlapping phenomenon of the spectrum and reduce the influence of scattered light on the spectrum. The most commonly used step size $\Delta\lambda$ (the difference between the emission wavelength (Em) and the excitation wavelength (Ex)) is 18 nm.[39,40,42]

The fluorescence spectra of the excitation and emission wavelengths of the four HAs are shown in Figure 3. The maximum Ex of the four HAs is about 270 nm, and the maximum Ems of the four HAs are in the range of 410−450 nm. The maximum Em of YLHA is 442.8 nm and the intensity is 34.05; the maximum Em of HBHA is 438.2 nm and the intensity is 44.73. The maximum Em of OYL is 445.5 nm, and the intensity is 22.74, which is slightly larger than the maximum Em of YLHA, and the intensity is lower, indicating that OYL has more electron-withdrawing groups (such as carboxyl and carbonyl). The maximum Em of OHB is 434.4 nm, and the intensity is 28.69, which is lower than the maximum Em and intensity of HBHA. The possible reason is that there are more electron-withdrawing groups (such as carboxyl and carbonyl) in OHB, which reduces its fluorescence intensity, and the unsaturated aliphatic structure or the aromatic system is reduced. At the same time, the reduction of the conjugated system in HAs makes the Em shift to the shortwave direction.

The synchronous fluorescence spectra of the four HAs are shown in Figure 4. It can be seen that YLHA has one obvious peak and two weaker small peaks, and HBHA has two obvious peaks, which indicates that YLHA has a simpler structure and minimal dispersion. When the Ex of the synchronous fluorescence spectrum ($\Delta\lambda$ = 18 nm) is in the range of 340−370 nm, the corresponding polycyclic aromatic hydrocarbons (PAHs) are composed of about three to four benzene rings; when Ex is in the range of 370−420 nm, the corresponding PAHs are composed of about five benzene rings; when Ex is in the range of 438−487 nm, the corresponding PAHs have about seven benzene rings or the molecule contains a lignin structure.[51] The PAHs in YLHA contain three to five benzene rings, and are mainly composed of five benzene rings. The PAHs in HBHA are mainly composed of three to four benzene rings, and YLHA and HBHA also contain a small amount of PAHs composed of seven benzene rings and/or lignin structures.

In the synchronous fluorescence spectrum of OYL, there is a relatively obvious peak in the Ex range of 340−420 nm, indicating that the PAHs in the molecule are mainly composed of three to five benzene rings. In the synchronous fluorescence spectrum of OHB, there is an obvious peak in the Ex range of 340−370 nm, and a small peak near 390 nm, indicating that the polycyclic aromatic hydrocarbons in the molecule are mainly composed of three to five benzene rings. In the Ex

https://doi.org/10.1021/acsomega.1c03257
ACS Omega 2021, 6, 24051−24061

Table 4. Fitted-Peak Results of FTIR Spectra of Four HAs (1800−1500 cm^{-1})[a]

attribution	YLHA		HBHA		OYL		OHB	
	λ	RP	λ	RP	λ	RP	λ	RP
carboxylic anhydride C═O stretching vibration	1770.1	0.98	1767.0	1.09	1770.0	1.58	1765.0	3.24
carboxyl C═O stretching vibration	1712.0	30.05	1714.0	25.13	1716.8	33.34	1714.5	33.29
carbonyl C═O stretching vibration	1663.0	3.97	1663.0	13.56	1660.0	9.67	1663.0	5.77
aromatic C═C vibration, C═CO vibration conjugated with carbonyl	1621.0	39.31	1613.0	33.92	1619.0	31.48	1617.5	36.41
COO-symmetrical stretching vibration	1560.0	18.01	1561.0	19.09	1561.0	20.23	1562.0	15.58
amide C═N stretching vibration, aromatic C═C deformation vibration	1509.0	7.68	1509.0	7.20	1504.5	3.74	1508.0	5.72

[a]Where λ is the wavenumber, cm^{-1}, and RP is the relative percentage, %.

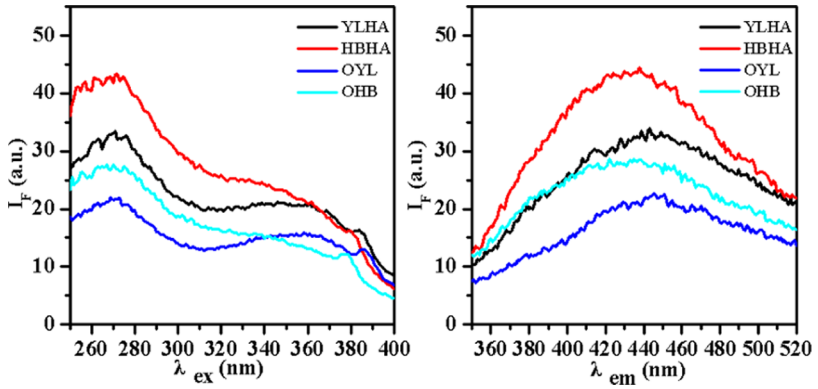

Figure 3. Excitation (left) and emission (right) spectra of four HAs.

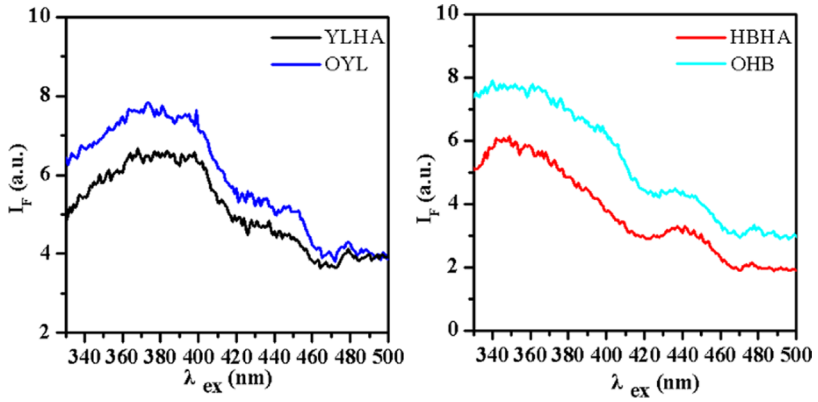

Figure 4. Synchronous fluorescence spectra of four HAs (Δλ = 18 nm).

range of 438−487 nm, OYL has a small peak near 450 and 480 nm, respectively, and OHB also has a small peak at 440 nm, indicating that there is a small amount of PAHs with seven benzene rings or lignin structures in both OYL and OHB molecules, similar to the YLHA and HBHA. It also can be seen that the synchronous fluorescence intensity of OYL and OHB is both larger than that of YLHA and HBHA, which may be related to the more C−O bond in OYL and OHB.

3.6. CP/MAS ^{13}C NMR Spectroscopy. CP/MAS ^{13}C NMR can be used to analyze the type of carbon in HAs, and nuclear magnetic data can be used to calculate the aromaticity, the aliphatic carbon ratio, and the hydrophilic−hydrophobic index ($f_{h/h}$) of HAs. Furthermore, the oxygen-containing functional group, the aliphatic structure, and the aromatic structure in HAs can be analyzed. In this paper, CP/MAS ^{13}C NMR is used to analyze the carbon types of four HAs, and the nuclear magnetic spectrum is shown in Figure 5.

The four samples showed an obvious peak in the range of 0−40 ppm, which belongs to aliphatic carbon. The strongest

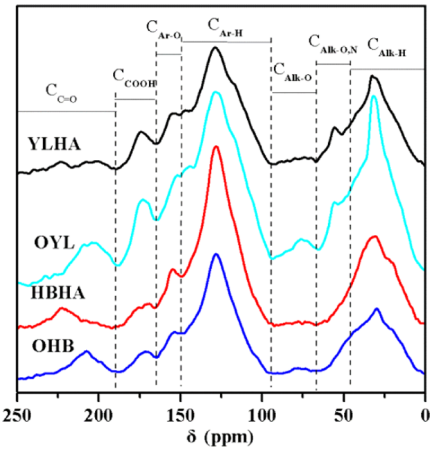

Figure 5. CP/MAS ^{13}C NMR spectra of four HAs.

https://doi.org/10.1021/acsomega.1c03257
ACS Omega 2021, 6, 24051−24061

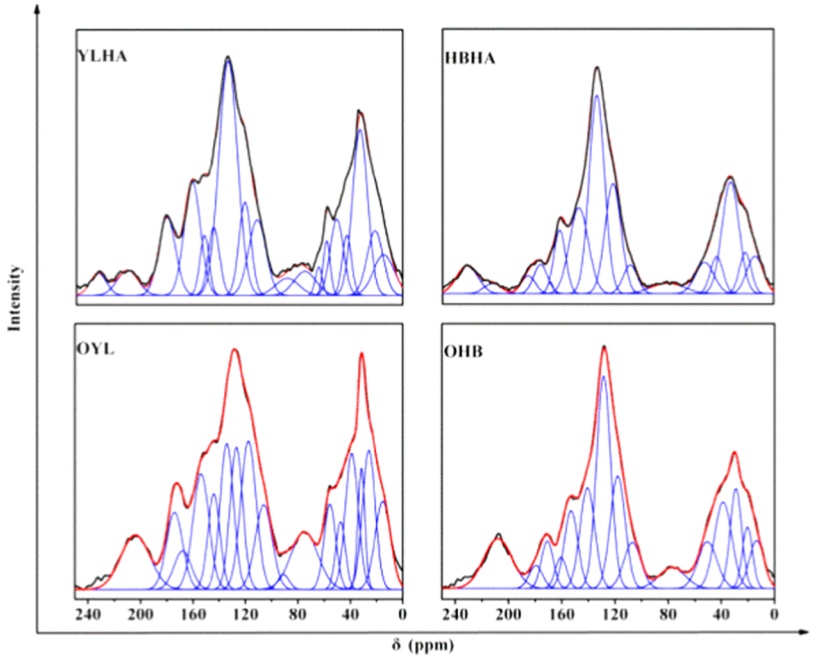

Figure 6. Fitted-peak curves of CP/MAS ^{13}C NMR spectra of four HAs.

Table 5. Fitted-Peak Results of CP/MAS ^{13}C NMR of Four HAs

	YLHA		HBHA		OYL		OHB	
attribution	δ	RP	δ	RP	δ	RP	δ	RP
aliphatic methyl carbon	14.00	4.35	13.50	4.58	15.20	5.94	13.50	4.39
	20.42	5.35	20.50	3.62	25.90	7.74	20.40	3.90
methylene carbon	31.50	12.72	31.20	14.11	31.65	3.64	29.00	7.08
polymethylene/alicyclic carbon	41.20	2.84	41.20	3.43	39.00	7.56	38.60	9.27
methoxy carbon	48.59	5.19	50.00	4.39	47.50	2.81	50.50	5.61
	56.00	1.94			55.60	4.32		
carbohydrates/oxygenated aliphatic carbon	61.81	1.00	77.00	2.59	75.00	6.66	77.00	3.42
	72.00	2.68			91.00	0.72		
	85.00	2.01						
proton aromatic carbon	107.00	6.69	104.00	3.05	106.00	6.12	107.00	4.88
	116.00	5.69	116.50	12.97	117.60	9.00	118.00	10.35
aromatic carbon	128.30	22.09	128.20	22.51	126.80	7.83	128.60	18.79
substituted aromatic carbon	139.00	4.02	141.20	12.02	134.10	8.46	140.70	9.27
	146.00	2.84			144.00	5.08		
phenolic carbon	155.00	9.37	155.10	5.57	154.00	8.10	153.00	6.59
			162.00	0.51			160.50	2.20
carboxy carbon	173.50	6.69	169.00	3.05	168.00	2.88	170.80	3.51
			178.00	1.87	174.20	5.40	179.50	1.95
carbonyl carbon	202.50	2.68	203.83	1.34	204.00	6.84	208.00	8.78
	224.00	1.84	222.16	4.39				

peak appears at 100−150 ppm, which is attributed to the aromatic carbon in HAs. It shows that the relative strength of OYL and OHB in the aliphatic carbon region (0−100 ppm) is higher than YLHA and HBHA, indicating that HAs extracted from oxidized lignites contain more aliphatic structures than that of raw lignites, while the aromatic structure is slightly decreased. The relative intensity of the aliphatic carbon region and the aromatic carbon region (100−150 ppm) of OYL is not much different, and the aromatic carbon content in OHB is more than the aliphatic carbon content. The peaks in the range of 165−190 ppm belong to the characteristic peaks of carboxyl groups. The intensity of the peaks of OYL and OHB in this range is greater than YLHA and HBHA, indicating that OYL and OHB contain a higher carboxyl content, and the results are consistent with the analysis results of FTIR.

To use CP/MAS ^{13}C NMR to quantitatively analyze HAs, the NMR spectrum of HAs was fitted by peaks. The fitted-peak curves of NMR spectra of four HAs are shown in Figure 6, and the corresponding attributions are shown in Table 5.

Compared with YLHA and HBHA, the aliphatic carbon content of OYL and OHB increases, while the aromatic carbon content decreases. The carboxyl content of OYL and OHB is higher than that of the corresponding HAs in raw lignites, which is consistent with the analysis results of oxygen-containing functional groups in Table 3. The hydroxyl carbon content of OYL phenol (8.1%) is lower than that of YLHA

https://doi.org/10.1021/acsomega.1c03257
ACS Omega 2021, 6, 24051−24061

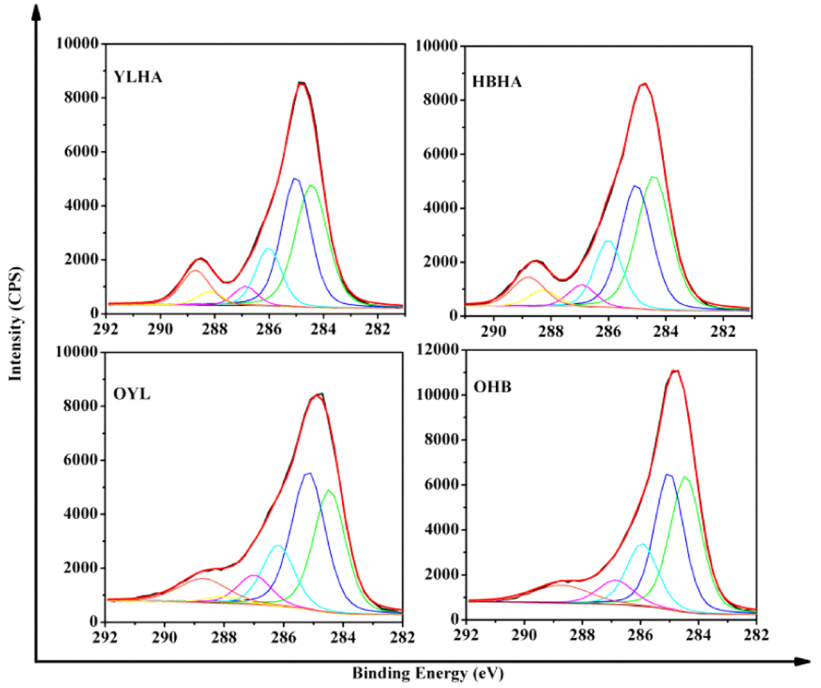

Figure 7. Fitted-peak curves of C 1s spectra of four HAs.

Table 6. Fitted-Peak Results of C 1s Spectra of Four HAs[a]

	aromatic carbon		aliphatic carbon		ether/alcohol carbon		ketone carbon		pyrrole/amide carbon		carboxyl carbon	
sample	BE	RP	BE	RP	BE	RP	BE	RP	BE	RP	BE	RP
YLHA	284.44	35.80	285.02	34.46	286.02	13.56	286.87	4.12	288.18	3.08	288.71	8.97
HBHA	284.42	36.49	285.04	31.73	286.00	15.09	286.93	4.95	288.28	3.95	288.79	7.79
OYL	284.46	30.35	285.17	36.10	286.18	15.12	286.99	7.48	288.02	1.76	288.73	9.20
OHB	284.44	35.11	285.02	33.10	285.94	16.09	286.85	7.28			288.71	8.41

[a]Where BE is binding energy (eV) and RP is relative proportion (%).

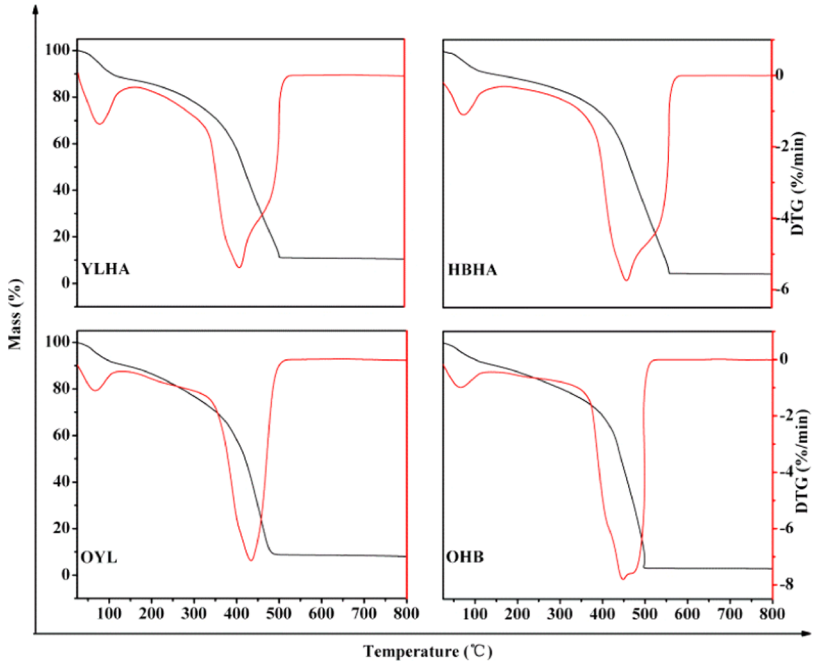

Figure 8. TG-DTG curves of four HAs.

https://doi.org/10.1021/acsomega.1c03257
ACS Omega 2021, 6, 24051−24061

Table 7. Mass Changes of Four HAs

	first stage	second stage	third stage	fourth stage	
sample	25−200 °C (%)	200−350 °C (%)	350−450 °C (%)	450−600 °C (%)	residue (%)
YLHA	14.22	14.43	36.24	24.25	10.86
HBHA	15.58	7.71	30.22	42.82	3.67
OYL	13.51	16.14	40.49	21.32	8.54
OHB	12.41	11.54	29.97	42.86	3.22

(9.37%). The possible reason is that phenol is converted into other substances during the oxidation process. The OHB phenolic hydroxyl carbon content (8.79%) is higher than that of HBHA (6.08%). The possible reason is that oxidation causes the −C−O bond between the benzene ring and the main structure to break. The content of carbonyl carbon in OYL is 6.84%, which is 2.32% higher than that of YLHA (4.52%). The content of carbonyl carbon in OHB is 8.78%, which is 3.05% higher than the content of carbonyl carbon in HBHA (5.73%), indicating that oxidation can oxidize alcohol ether phenolic compounds in HA molecules to ketones or carbonyl compounds.

The oxygen-containing and nitrogen-containing alkyl carbons in HAs were hydrophilic carbons, which affect the biological activity of HAs. The hydrophilic/hydrophobic indexes ($f_{h/h}$)[52] of four HAs are calculated according to eq 2, and the results are listed in Table 3.

$$f_{h/h} = \frac{C_{C=O} + C_{COOH} + C_{Ar-OH} + C_{O-Alk-O} + C_{Alk-O}}{C_{Alk} + C_{Ar}} \quad (2)$$

It can be seen from Table 3 that the $f_{h/h}$ of the four samples is OYL > YLHA > OHB > HBHA, indicating that OYL has the most hydrophilic groups, and in agricultural applications, OYL has higher biological activity.[52] It shows that HAs extracted from oxidized lignites contain more hydrophilic groups than those of raw lignites, indicating that oxidation can improve the biological activity of HAs.

3.7. XPS Spectrometry. XPS spectrometry is an analytical method used to measure the surface elements of samples. This paper uses XPS to analyze the surface carbon and oxygen elements of four HAs. When using XPS to analyze the surface carbon of HAs, there are six main chemical states, including aromatic carbon, aliphatic carbon, ether/alcohol carbon, ketone carbon, pyrrole/amide carbon, and carboxyl carbon.[4] The C 1s of the XPS of the four HAs were fitted by peaks. The fitting results are shown in Figure 7, and the fitting results are shown in Table 6.

The main existing forms of carbon elements on the surface of four HAs are aromatic carbon and aliphatic carbon. Compared with the YLHA and HBHA, it can be found that the aromatic carbon content of OYL and OHB is lower, and the aliphatic carbon content is higher. The contents of ether/alcohol carbon, ketone carbon, and carboxyl carbon of OYL and OHB are larger than YLHA and HBHA, respectively, indicating that oxidation can increase the oxygen-containing functional groups in HAs, and can oxidize alcohol ether phenolic compounds into ketones, carbonyls, and carboxylic acid compounds. The analysis results are consistent with the NMR results.

3.8. TG-DTG Analysis. The results of TG-DTG analysis of the four HAs are shown in Figure 8. The TG and DTG curves of the four HAs are similar. From the TG curves, it can be seen that the HAs always suffer from quality loss when the temperature increases from 20 °C, and the maximum weight loss rate appears in the temperature ranges of 20−120, 350−450, and 450−600 °C, indicating that there is greater loss in the quality of HAs in these three temperature ranges, respectively.

The weight loss of HAs can be divided into four stages. The first stage is 20−200 °C, which is attributed to the evaporation of free water and bound water in the HAs, and the decomposition of some small molecular weight organic matters.[53] The second stage is 200−350 °C; the mass loss in this stage is mainly caused by the degradation of sugar compounds in the samples, the dehydration of aliphatic alcohols, and the decomposition of functional groups such as carboxyl, phenolic hydroxyl, and carbonyl.[53−55] The third stage is 350−450 °C. The quality loss in this stage is attributed to the degradation of more polycondensation structures, the breaking of C−C bonds, the oxidation of aromatic components, etc., which are mainly related to the occurrence of long-chain hydrocarbons and nitrogen-containing compounds.[33] The fourth stage is 450−600 °C; the quality loss of this stage is caused by the pyrolysis of the aromatic components in the structure of lignin and other polyphenols, and the destruction of the aromatic structure in HAs.[54] Therefore, the relative mass losses of the four HAs at the corresponding stages are listed in Table 7.

It can be seen that in the range of 200−350 °C, the quality loss of OYL and OHB is greater than that of YLHA and HBHA, respectively, indicating that the HAs of oxidized lignite contain more oxygen-containing functional groups and aliphatic structures, which are consistent with the analysis results of ultimate analysis, acid functional group determination, and NMR. The temperature of the peak of maximum weight loss on the DTG curves of OYL and OHB is higher than that of YLHA and HBHA, indicating that the thermal oxidation of HAs extracted from oxidized lignites is better.[37] In addition, OYL is decomposed at about 484 °C, which is lower than the decomposition temperature of YLHA (508 °C), and OHB is decomposed at about 500 °C, which is lower than the decomposition temperature of HBHA (539 °C). It shows that the heat resistance of HAs extracted from oxidized lignites is worse than that of HAs extracted from raw lignites, which is related to the less aromatic structure in HAs extracted from oxidized lignites.[56]

4. CONCLUSIONS AND FUTURE DIRECTIONS

The HA content of YL lignite under the optimal oxidation condition is 17.6% higher than that of raw lignite (27.8%), and that of HB lignite under the optimal oxidation condition is 17.0% higher than that of raw lignite (23.9%). Through ultimate analysis, it is concluded that the carbon content of HAs extracted from the oxidized lignites reduces and the oxygen content increases. According to the determination of acid functional groups, FTIR analysis, and CP/MAS ^{13}C NMR analysis, the HAs extracted from oxidized lignites contain more

https://doi.org/10.1021/acsomega.1c03257
ACS Omega 2021, 6, 24051−24061

carboxyl groups, C−O groups, and total acidic groups than those extracted from raw lignites, and the functional groups and structures of HAs are similar.

Through CP/MAS ^{13}C NMR and XPS analysis, the HAs extracted from oxidized lignites contain more aliphatic carbon and less aromatic carbon than that extracted from raw lignites. The content of ether/alcohol carbon, ketone carbon, and carboxyl carbon and the $f_{h/h}$ value of HAs extracted from oxidized lignites are all higher than those of HAs extracted from raw lignites.

According to TG-DTG analysis, the HAs extracted from oxidized lignite have the decomposition of moisture, oxygen-containing functional groups, the aliphatic structure and the aromatic structure, and have better thermal oxidation property but worse heat resistance than that of HAs extracted from raw lignites. The structure, dispersibility, and fluorophore types of HAs extracted from oxidized lignites are similar to those extracted from raw lignites by fluorescence analysis.

The abovementioned studies show that the oxidation of H_2O_2 can increase the oxygen-containing functional groups in HAs, and the alcohol−ether phenolic compounds in molecules of HAs can be oxidized into ketones or carbonyl compounds, indicating that the oxidation can improve the biological activity of HAs. The future research can focus on the application of HAs and make in-depth exploration by comparing the application effects of HAs extracted from lignites before and after oxidation; the mechanism of oxidation reaction and its molecular structure also can be discussed more so as to provide new ideas for the application of lignites with a high-added value.

AUTHOR INFORMATION

Corresponding Author

Yanhong Li − *Faculty of Chemical Engineering, Kunming University of Science and Technology, Kunming, Yunnan 650500, China;* orcid.org/0000-0001-6434-2761; Email: liyh_2004@163.com

Authors

Miao Wang − *Faculty of Chemical Engineering, Kunming University of Science and Technology, Kunming, Yunnan 650500, China*

Yuanqin Zhang − *Faculty of Chemical Engineering, Kunming University of Science and Technology, Kunming, Yunnan 650500, China*

Xun Hu − *School of Material Science and Engineering, University of Jinan, Jinan 250022, China;* orcid.org/0000-0003-4329-2050

Qingyin Li − *School of Material Science and Engineering, University of Jinan, Jinan 250022, China*

Yi Su − *Faculty of Chemical Engineering, Kunming University of Science and Technology, Kunming, Yunnan 650500, China*

Wenbo Zhao − *Faculty of Chemical Engineering, Kunming University of Science and Technology, Kunming, Yunnan 650500, China;* orcid.org/0000-0003-3119-9342

Complete contact information is available at: https://pubs.acs.org/10.1021/acsomega.1c03257

Notes

The authors declare no competing financial interest.

ACKNOWLEDGMENTS

The authors thank the financial supports provided by the National Natural Science Foundation of China (21766013) and the Analysis and Testing Foundation of Kunming University of Science and Technology (2020M20192208013).

REFERENCES

(1) Liu, F. J.; Wei, X. Y.; Fan, M.; Zong, Z. M. Separation and structural characterization of the value-added chemicals from mild degradation of lignites: A review. *Appl. Energy* **2016**, *170*, 415−436.

(2) Li, Z. K.; Wei, X. Y.; Yan, H. L.; Zong, Z. M. Insight into the structural features of Zhaotong lignite using multiple techniques. *Fuel* **2015**, *153*, 176−182.

(3) Murata, S.; Hosokawa, M.; Kidena, K.; Nomura, M. Analysis of oxygen-functional groups in brown coals. *Fuel Process. Technol.* **2000**, *67*, 231−243.

(4) Doskočil, L.; Burdíková-Szewieczková, J.; Enev, V.; Kalina, L.; Wasserbauer, J. Spectral characterization and comparison of humic acids isolated from some European lignites. *Fuel* **2018**, *213*, 123−132.

(5) Zhang, Y.; Li, Y.; Chang, L.; Zi, C.; Liang, G.; Zhang, D.; Su, Y. A comparative study on the structural features of humic acids extracted from lignites using comprehensive spectral analyses. *RSC Adv.* **2020**, *10*, 22002−22009.

(6) Wang, C. F.; Fan, X.; Zhang, F.; Wang, S. Z.; Zhao, Y. P.; Zhao, X. Y.; Zhao, W.; Zhu, T. G.; Lu, J. L.; Wei, X. Y. Characterization of humic acids extracted from a lignite and interpretation for the mass spectra. *RSC Adv.* **2017**, *7*, 20677−20684.

(7) Gong, G. Q.; Zhao, Y. F.; Zhang, Y. J.; Deng, B.; Liu, W. X.; Wang, M.; Yuan, X.; Xu, L. W. Establishment of a molecular structure model for classified products of coal-based fulvic acid. *Fuel* **2020**, *267*, No. 117210.

(8) Ou, X.; Chen, S.; Xie, Q.; Zhao, H. Photochemical activity and characterization of the complex of humic acids with iron(III). *J. Geochem. Explor.* **2009**, *102*, 49−55.

(9) Havelcová, M.; Mizera, J.; Sykorová, I.; Peka, M. Sorption of metal ions on lignite and the derived humic substances. *J. Hazard. Mater.* **2009**, *161*, 559−564.

(10) Qian, S.; Ding, W.; Li, Y.; Liu, G.; Sun, J.; Ding, Q. Characterization of humic acids derived from Leonardite using a solid-state NMR spectroscopy and effects of humic acids on growth and nutrient uptake of snap bean. *Chem. Speciation Bioavailability* **2015**, *27*, 156−161.

(11) Rose, M. T.; Patti, A. F.; Little, K. R.; Brown, A. L.; Jackson, W. R.; Cavagnaro, T. R. A Meta-Analysis and Review of Plant-Growth Response to Humic Substances. *Adv. Agron.* **2014**, *124*, 37−89.

(12) Tahiri, A.; Richel, A.; Destain, J.; Druart, P.; Thonart, P.; Ongena, M. Comprehensive comparison of the chemical and structural characterization of landfill leachate and leonardite humic fractions. *Anal. Bioanal. Chem.* **2016**, *408*, 1917−1928.

(13) Huang, G.; Kang, W.; Xing, B.; Chen, L.; Zhang, C. Oxygen-rich and hierarchical porous carbons prepared from coal based humic acid for supercapacitor electrodes. *Fuel Process. Technol.* **2016**, *142*, 1−5.

(14) Sun, Z.; Tang, B.; Xie, H. Treatment of Waste Gases by Humic Acid. *Energy Fuels* **2015**, *29*, 1269−1278.

(15) Paul, B.; Parashar, V.; Mishra, A. Graphene in the Fe_3O_4 nanocomposite switching the negative influence of humic acid coating into an enhancing effect in the removal of arsenic from water. *Environ. Sci.: Water Res. Technol.* **2015**, *1*, 77−83.

(16) Zingaretti, D.; Lominchar, M. A.; Verginelli, I.; Santos, A.; Baciocchi, R. Humic acids extracted from compost as amendments for Fenton treatment of diesel-contaminated soil. *Environ. Sci. Pollut. Res.* **2020**, *27*, 22225−22234.

(17) de Melo, B. A. G.; Motta, F. L.; Santana, M. Humic acids: Structural properties and multiple functionalities for novel technological developments. *Mater. Sci. Eng., C* **2016**, *62*, 967−974.

(18) Zykova, M. V.; Schepetkin, I. A.; Belousov, M. V.; Krivoshchekov, S. V.; Logvinova, L. A.; Bratishko, K. A.; Yusubov,

M. S.; Romanenko, S. V.; Quinn, M. T. Physicochemical Characterization and Antioxidant Activity of Humic Acids Isolated from Peat of Various Origins. *Molecules* **2018**, *23*, No. 753.
(19) El-Zaiat, H. M.; Morsy, A. S.; El-Wakeel, E. A.; Anwer, M. M.; Sallam, S. M. Impact of humic acid as an organic additive on ruminal fermentation constituents, blood parameters and milk production in goats and their kids growth rate. *J. Anim. Feed Sci.* **2018**, *27*, 105−113.
(20) Penamendez, E. M.; Havel, J.; Patocka, J. Humic substances - compounds of still unknown structure: applications in agriculture, industry, environment, and biomedicine. *J. Appl. Biomed.* **2005**, *33*, 279−288.
(21) Sarlaki, E.; Asp, B.; Mhk, A.; Kav, A. Valorization of lignite wastes into humic acids: Process optimization, energy efficiency and structural features analysis. *Renewable Energy* **2021**, *163*, 105−122.
(22) Haider, R.; Ghauri, M. A.; Akhtar, K. Isolation of Coal Degrading Fungus from Drilled Core Coal Sample and Effect of Prior Fungal Pretreatment on Chemical Attributes of Extracted Humic Acid. *Geomicrobiol. J.* **2015**, *32*, 944−953.
(23) Gong, G.; Yuan, X.; Zhang, Y.; Li, Y.; Liu, W.; Wang, M.; Zhao, Y.; Xu, L. Characterization of coal-based fulvic acid and the construction of a fulvic acid molecular model. *RSC Adv.* **2020**, *10*, 5468−5477.
(24) Tahmasebi, A.; Jiang, Y.; Yu, J.; Li, X.; Lucas, J. Solvent extraction of Chinese lignite and chemical structure changes of the residue during H_2O_2 oxidation. *Fuel Process. Technol.* **2015**, *129*, 213−221.
(25) Vlčková, Z.; Grasset, L.; Antošová, B.; Pekař, M.; Kučerík, J. Lignite pre-treatment and its effect on bio-stimulative properties of respective lignite humic acids. *Soil Biol. Biochem.* **2009**, *41*, 1894−1901.
(26) Fong, S. S.; Seng, L.; Mat, H. B. Reuse of nitric acid in the oxidative pretreatment step for preparation of humic acids from low rank coal of Mukah, Sarawak. *J. Braz. Chem. Soc.* **2007**, *18*, 41−46.
(27) Doskočil, L.; Grasset, L.; Válková, D.; Pekař, M. Hydrogen peroxide oxidation of humic acids and lignite. *Fuel* **2014**, *134*, 406−413.
(28) Zhou, L.; Yuan, L.; Zhao, B.; Li, Y.; Lin, Z. Structural characteristics of humic acids derived from Chinese weathered coal under different oxidizing conditions. *PLoS One* **2019**, *14*, No. e0217469.
(29) Erdogan, S.; Duz, M.; Merdivan, M.; Hamamci, C. Formation And Characterization Of Humic Acids From Low Rank Anatolian Coals By Air Oxidation. *Energy Sources* **2005**, *27*, 423−430.
(30) Savel'Eva, A. V.; Ivanov, A. A.; Yudina, N. V.; Lomovskii, O. I. Composition and properties of humic acids from natural and mechanochemically oxidized brown coal. *Solid Fuel Chem.* **2015**, *49*, 201−205.
(31) Tang, Y.; Yang, Y.; Cheng, D.; Gao, B.; Wan, Y.; Li, Y. C. Value-Added Humic Acid Derived from Lignite Using Novel Solid-Phase Activation Process with Pd/CeO_2 Nanocatalyst: A Physiochemical Study. *ACS Sustainable Chem. Eng.* **2017**, *5*, 10099−10110.
(32) Liu, F. J.; Zong, Z. M.; Gui, J.; Zhu, X. N.; Wei, X. Y.; Bai, L. Selective production and characterization of aromatic carboxylic acids from Xianfeng lignite-derived residue by mild oxidation in aqueous H_2O_2 solution. *Fuel Process. Technol.* **2018**, *181*, 91−96.
(33) Huculak-Mczka, M.; Hoffmann, J.; Hoffmann, K. Evaluation of the possibilities of using humic acids obtained from lignite in the production of commercial fertilizers. *J. Soils Sediments* **2018**, *18*, 2868−2880.
(34) Sarlaki, E.; Paghaleh, A. S.; Kianmehr, M. H.; Vakilian, K. A. Chemical, Spectral and Morphological Characterization of Humic Acids Extracted and Membrane Purified from Lignite. *Chem. Chem. Technol.* **2020**, *14*, 353−361.
(35) Francioso, O.; Ciavatta, C.; Montecchio, D.; Tugnoli, V.; Sanchez-Cortes, S.; Gessa, C. Quantitative estimation of peat, brown coal and lignite humic acids using chemical parameters, ^{1}H-NMR and DTA analyses. *Bioresour. Technol.* **2003**, *88*, 189−195.
(36) Nasir, S.; Sarfaraz, T. B.; Verheyen, T. V.; Chaffee, A. L. Structural elucidation of humic acids extracted from Pakistani lignite using spectroscopic and thermal degradative techniques. *Fuel Process. Technol.* **2011**, *92*, 983−991.
(37) Francioso, O.; Montecchio, D.; Gioacchini, P.; Ciavatta, C. Thermal analysis (TG-DTA) and isotopic characterization (^{13}C-^{15}N) of humic acids from different origins. *Appl. Geochem.* **2005**, *20*, 537−544.
(38) Peuravuori, J.; Žbánková, P.; Pihlaja, K. Aspects of structural features in lignite and lignite humic acids. *Fuel Process. Technol.* **2006**, *87*, 829−839.
(39) Fuentes, M.; González-Gaitano, G.; García-Mina, J. The usefulness of UV−visible and fluorescence spectroscopies to study the chemical nature of humic substances from soils and composts. *Org. Geochem.* **2006**, *37*, 1949−1959.
(40) Enev, V.; Pospíšilová, L.; Klucakova, M.; Liptaj, T.; Doskocil, L. Spectral characterization of selected humic substances. *Soil Water Res.* **2014**, *9*, 9−17.
(41) Cheng, G.; Niu, Z.; Zhang, C.; Zhang, X.; Li, X. Extraction of Humic Acid from Lignite by KOH-Hydrothermal Method. *Appl. Sci.* **2019**, *9*, No. 1356.
(42) Rodríguez, F. J.; Schlenger, P.; García-Valverde, M. A comprehensive structural evaluation of humic substances using several fluorescence techniques before and after ozonation. Part I: Structural characterization of humic substances. *Sci. Total Environ.* **2014**, *476*−*477*, 718−730.
(43) Chen, W.; Yu, H. Q. Advances in the characterization and monitoring of natural organic matter using spectroscopic approaches. *Water Res.* **2020**, *190*, No. 116759.
(44) Xiong, Y. K.; Jin, L. J.; Yang, H.; Li, Y.; Hu, H. Q. Insight into the aromatic ring structures of a low-rank coal by step-wise oxidation degradation. *Fuel Process. Technol.* **2020**, *210*, No. 106563.
(45) Zhang, Y. J.; Gong, G. Q.; Zheng, H. L.; Yuan, X.; Xu, L. W. Synergistic Extraction and Characterization of Fulvic Acid by Microwave and Hydrogen Peroxide-Glacial Acetic Acid to Oxidize Low-Rank Lignite. *ACS Omega* **2020**, *5*, 6389−6394.
(46) Wang, M. H.; Wang, R. Y.; Wei, X. Y.; Zhao, W.; Fan, X. Molecular characteristics of the oxidation products of a lignite based on the big data obtained from Fourier transform ion cyclotron resonance mass spectrometry. *Fuel* **2021**, *295*, No. 120644.
(47) Xiong, Y. K.; Jin, L. J.; Li, Y.; Zhu, J. L.; Hu, H. Q. Hydrogen peroxide oxidation degradation of a low-rank Naomaohu coal. *Fuel Process. Technol.* **2020**, *207*, No. 106484.
(48) Allard, B. A comparative study on the chemical composition of humic acids from forest soil, agricultural soil and lignite deposit. Bound lipid, carbohydrate and amino acid distributions. *Geoderma* **2006**, *130*, 77−96.
(49) Dick, D. P.; Mangrich, A. S.; Menezes, S.; Pereira, B. F. Chemical and Spectroscopical Characterization of Humic Acids from two South Brazilian Coals of Different Ranks. *J. Braz. Chem. Soc.* **2002**, *13*, 177−182.
(50) Novák, F.; Šestauberová, M.; Hrabal, R. Structural features of lignohumic acids. *J. Mol. Struct.* **2015**, *1093*, 179−185.
(51) Peuravuori, J.; Koivikko, R.; Pihlaja, K. Characterization, differentiation and classification of aquatic humic matter separated with different sorbents: synchronous scanning fluorescence spectroscopy. *Water Res.* **2002**, *36*, 4552−4562.
(52) Zherebtsov, S. I.; Malyshenko, N. V.; Votolin, K. S.; Androkhanov, V. A.; Sokolov, D. A.; Dugarjav, J.; Ismagilov, Z. R. Structural-Group Composition and Biological Activity of Humic Acids Obtained from Brown Coals of Russia and Mongolia. *Solid Fuel Chem.* **2019**, *53*, 145−151.
(53) DAS, T.; SAIKIA, B. K.; BARUAH, B. P.; DAS, D. Characterizations of humic acid isolated from coals of two Nagaland Coalfields of India in relation to their origin. *J. Geol. Soc. India* **2015**, *86*, 468−474.
(54) Xavier, D. M.; Silva, A. S.; Santos, R. P.; Mesko, M. F.; Costa, S. N.; Freire, V. N.; Cavada, B. S.; Martins, J. L. Characterization of the Coal Humic Acids from the Candiota Coalfield, Brazil. *Int. J. Agric. Sci.* **2012**, *4*, 238−242.

https://doi.org/10.1021/acsomega.1c03257
ACS Omega 2021, 6, 24051−24061

(55) Giovanela, M.; Parlanti, E.; Soriano-Sierra, E. J.; Soldi, M. S.; Sierra, M. Elemental compositions, FT-IR spectra and thermal behavior of sedimentary fulvic and humic acids from aquatic and terrestrial environments. *Geochem. J.* **2004**, *38*, 255−264.
(56) Giovanela, M.; Crespo, J. S.; Antunes, M.; Adamatti, D. S.; Fernandes, A. N.; Barison, A.; Silva, C.; Guégan, R.; Motelica-Heino, M.; Sierra, M. Chemical and spectroscopic characterization of humic acids extracted from the bottom sediments of a Brazilian subtropical microbasin. *J. Mol. Struct.* **2010**, *981*, 111−119.

https://doi.org/10.1021/acsomega.1c03257
ACS Omega 2021, 6, 24051−24061